Evaluation of ^{64}Cu-ATSM In Vitro and In Vivo in a Hypoxic Tumor Model

Jason S. Lewis, Deborah W. McCarthy, Timothy J. McCarthy, Yasuhisa Fujibayashi and Michael J. Welch

Mallinckrodt Institute of Radiology, Washington University School of Medicine, St. Louis, Missouri; Biomedical Imaging Research Center, Fukui Medical University, Matsuoka, Fukui, Japan

We have evaluated Cu-diacetyl-bis(N^4-methylthiosemicarbazone) (Cu-ATSM), an effective marker for the delineation of hypoxic but viable tissue, in vitro in the EMT6 carcinoma cell line under varying degrees of hypoxia and compared it with the flow tracer ^{64}Cu-pyruvaldehyde-bis(N^4-methylthiosemicarbazone) (Cu-PTSM) and the hypoxic tracer ^{18}F-fluoromisonidazole (MISO). We have also compared the uptake of Cu-ATSM and Cu-PTSM in vivo and ex vivo in a murine animal model bearing the EMT6 tumor. **Methods:** Uptake of ^{64}Cu-ATSM, ^{64}Cu-PTSM and ^{18}F-MISO in vitro into EMT6 cells was investigated at the dissolved oxygen concentrations of 0, 1×10^3, 5×10^3, 5×10^4 and 2×10^5 ppm. Biodistribution performed at 1, 5, 10, 20 and 40 min compared ^{64}Cu-ATSM with ^{64}Cu-PTSM in BALB/c mice bearing EMT6 tumors. To determine long-term retention of ^{64}Cu-ATSM, biodistribution was also performed at 1, 2 and 4 h. Ex vivo autoradiography of tumor slices after co-injection of ^{60}Cu-PTSM (^{60}Cu, $T_{1/2}$ = 23.7 min) and ^{64}Cu-ATSM (^{64}Cu, $t_{1/2}$ = 12.7 h) into the same animal was performed. **Results:** After 1 h, ^{64}Cu-ATSM was taken up by EMT6 cells: 90% at 0 ppm, 77% at 1×10^3 ppm, 38% at 5×10^3 ppm, 35% at 5×10^4 ppm and 31% at 2×10^5 ppm. ^{18}F-MISO also showed oxygen concentration dependent uptake, but with lower percentages than ^{64}Cu-ATSM. ^{64}Cu-PTSM showed 83%–85% uptake into the cells after 1 h, independent of oxygen concentration. Biodistribution data of ^{64}Cu-ATSM and ^{64}Cu-PTSM showed optimal tumor uptake after 5 and 10 min, respectively (0.76% injected dose (ID)/organ for ^{64}Cu-ATSM and 1.11%ID/organ for ^{64}Cu-PTSM). Ex vivo imaging experiments showed ^{60}Cu-PTSM uniform throughout the EMT6 tumor, but heterogeneous uptake of ^{64}Cu-ATSM, indicative of selective trapping of ^{64}Cu-ATSM into the hypoxic tumor cells. **Conclusion:** Cu-ATSM exhibits selectivity for hypoxic tumor tissue both in vivo and in vitro and may provide a successful diagnostic modality for the detection of tumor ischemia.

Key Words: hypoxia; ^{64}Cu; ^{60}Cu; ATSM; EMT6

J Nucl Med 1999; 40:177–183

Resistance of tumors to conventional therapies can seriously affect the successful management of cancer. Hypoxic cells within the tumor can account, in part, for this resistance to radiotherapy (*1,2*) and chemotherapy (*3–5*). A noninvasive, quantitative PET imaging agent could measure the extent of tumor hypoxia before a treatment regimen. Misonidazole derivatives have been labeled with ^{18}F for PET imaging; clinical studies involving the lead compound, ^{18}F-fluoromisonidazole (MISO), show imageable differences between normal and hypoxic tissues. Misonidazole analogs and 2-nitroimidazole functionalities have also been labeled with ^{123}I (*6–10*) for SPECT imaging. The ^{99m}Tc compounds, ^{99m}Tc-HL91 and BMS-181321, have demonstrated increased uptake in hypoxic and low-flow ischemic myocardium (*8,9*) and in tumors (*11,12*).

The production and use of the positron emitting isotopes of copper (^{60}Cu, ^{61}Cu, ^{62}Cu and ^{64}Cu) in nuclear medicine have been reviewed (*13*). Cu-diacetyl-bis(N^4-methylthiosemicarbazone) (ATSM) has been shown to be an effective marker for delineating hypoxic, viable tissue; it is selectively trapped in hypoxic tissue but rapidly washed out from normoxic cells (*14,15*). ^{62}Cu-ATSM is currently under investigation in humans at Fukui Medical Center, Japan, for the detection of ischemia (*16*). In addition, ^{60}Cu-ATSM is approved at Washington University Medical School, St. Louis, for the clinical diagnosis of tumor hypoxia in lung cancer.

With the availability of high specific activity positron emitting isotopes of copper from a biomedical cyclotron (*17*), we have evaluated ^{64}Cu-ATSM in vitro with the EMT6 cell line under varying pO_2 and in vivo in a murine animal model.

MATERIALS AND METHODS

^{64}Cu and ^{60}Cu were produced on the Cyclotron Corporation CS15 cyclotron at the Washington University Medical School as previously described (*17,18*). ^{18}F-MISO was synthesized according to procedures by McCarthy et al. (*19*). Female BALB/c mice were purchased from Charles River Laboratories (Wilmington, MA). All chemicals unless otherwise stated were purchased from Aldrich Chemical Company, Inc. (Milwaukee, WI). All solutions were prepared with distilled deionized water (Milli-Q; >18 MΩ resistivity). Thin-layer chromatography (TLC) was performed by using silica gel TLC plates with ethyl acetate as the mobile phase. TLC plates were analyzed on a BIOSCAN System 200 imaging scanner (Washington, DC). Radioactive samples were counted on a Beckman 8000 gamma counter (Irvine, CA). Tumor slices were prepared in Tissue-Tek Embedding Medium (Miles, Inc., Elkhart,

Received Mar. 9, 1998; revision accepted May 21, 1998.

For correspondence and requests for reprints contact: Michael J. Welch, PhD, Mallinckrodt Institute of Radiology, Washington University School of Medicine, Campus Box 8225, 510 S. Kingshighway Blvd., St. Louis, MO 63110.

IN). Electronic autoradiography was performed on an InstantImager Electronic Autoradiography System (Packard Instrument Co., Meriden, CT) (*20*). The mouse mammary tumor line EMT6 was obtained from the laboratories of Dr. Ronald S. Pardini at the University of Nevada, Reno, and maintained by serial passage in cell culture. Oxygen concentration during the in vitro studies was monitored by an Oxygen Transmitter (Model 4300) and Oxygen Sensor from Mettler Toledo (Wilmington, MA).

Radiochemical Synthesis

^{64}Cu-ATSM, ^{64}Cu-pyruvaldehyde-bis(*N**-methylthiosemicarbazone) (^{64}Cu-PTSM) and ^{60}Cu-PTSM were produced by methods identical to literature procedures (*20,21*). The compounds were produced at 1×10^{-2} MBq/μg.

Uptake of Radiolabeled Compounds into EMT6 Cells

The apparatus and procedures for the in vitro experiments are based on methods previously described (*22,23*). Viability of the cells and cell numbers was measured with a hemocytometer according to trypan blue exclusion procedures. The EMT6 cells ($1.2–1.4 \times 10^6$ cells/mL) were equilibrated in a glass round-bottomed flask at a maintained temperature of 37°C. A continual flow of warmed, humidified gas (20% O_2, 5% CO_2, 75% N_2 [control]; 5% O_2, 5% CO_2, 90% N_2 [hypoxia]; 0.5% O_2, 5% CO_2, 94.5% N_2 [hypoxia]; 0.1% O_2, 5% CO_2, 94.9% N_2 [hypoxia]; 0% O_2, 5% CO_2, 95% N_2 [anoxia]) was passed over the cells. The pO_2 and temperature were monitored by an oxygen probe. After equilibration, 7.4 MBq (200 μCi) (0.15 μg) ^{64}Cu-ATSM (0.15 μg), ^{64}Cu-PTSM (0.15 μg) or ^{18}F-MISO were added to the cells. At 1, 5, 15, 30, 45 and 60 min, triplicate aliquots were removed. The cells were pelleted from the media, and the percentage uptake of the compound into the cells was calculated. Cell viability was >96%.

Additional experiments examined the uptake of ^{18}F-MISO at higher cell concentrations (5.0×10^6 cells/mL). Monolayers of EMT6 cells were gassed with the required gas mixture in cell culture flasks. The flasks were kept at 37°C and, after 1 h, 7.4 MBq (200 μCi) ^{18}F-MISO were added. Oxygen concentration was constantly monitored. After 2 h, the cells were separated and washed to calculate percentage uptake.

Retention of Radiolabeled Compounds in EMT6 Cells

The washout of radioactivity from the cells was observed by obtaining a cell pellet after 1 h incubation with the radiolabeled compounds and resuspending it in fresh media. The fully oxygenated gas mixture was blown over the cells (20% O_2). Samples were taken at 1, 5, 15, 30, 45 and 60 min postresuspension.

Animal Biodistribution Studies

All animal experiments were conducted in compliance with the Guidelines for the Care and Use of Research Animals established by Washington University's Animal Studies Committee.

BALB/c mice were implanted subcutaneously into each flank with 2.0×10^5 EMT6 cells from cell culture. At 10 days (tumors approximately 0.4–0.5 g), ^{64}Cu-ATSM (0.2 MBq [5 μCi]) or ^{64}Cu-PTSM (0.2 MBq [5 μCi]) was injected into the tail vein and the animals were euthanized by cervical dislocation at 1, 5, 10, 20 and 40 min (ATSM and PTSM) and at 1, 2 and 4 h postinjection (ATSM only) (n = 4). Selected tissues and organs were harvested and weighed, and the activity counted on the gamma counter. The percentage injected dose per gram (%ID/g) and percentage injected dose per organ (%ID/organ) for each tissue were calculated.

Electronic Autoradiography

EMT6 cells (2.5×10^5) from cell culture were implanted subcutaneously into each flank of 5 BALB/c mice. At 9 d (tumors approximately 0.25g), the mice were co-injected with 5.5 MBq (150 μCi) ^{60}Cu-ATSM and 0.2 MBq (5 μCi) ^{64}Cu-PTSM, in saline, into the tail vein. The animals were killed by cervical dislocation after 10 min and the tumors excised. Slices (1 mm thick) were mounted and placed in the electronic autoradiography system 5 h after the initial scan to localize ^{60}Cu-PTSM; a second scan visualized distribution of ^{64}Cu-ATSM.

RESULTS

In Vitro Studies

The uptake of ^{64}Cu-ATSM into EMT6 cells was investigated as a function of pO_2 at fixed temperature (37°C), pH and cell concentration. At 1 min, between 8% and 14% of ^{64}Cu-ATSM was associated with the EMT6 cells over the whole range of pO_2. By 1 h, the percentage uptake of ^{64}Cu-ATSM into the cells was significantly different depending on pO_2 (Fig. 1A). The uptake of ^{64}Cu-ATSM is shown as a function of pO_2 (in ppm) at 1 h in Figure 2A.

^{64}Cu-PTSM was more rapidly and efficiently taken up by EMT6 cells after 1 min (76%–82%), independent of the pO_2. In addition, this uptake was maintained over the experiment (83%–85% at 1 h) (Fig. 1B).

^{18}F-MISO uptake was not detected when suspended cells were used. Therefore, uptake was studied in monolayers of cells at higher concentrations (5.0×10^6 cells/mL). After 2

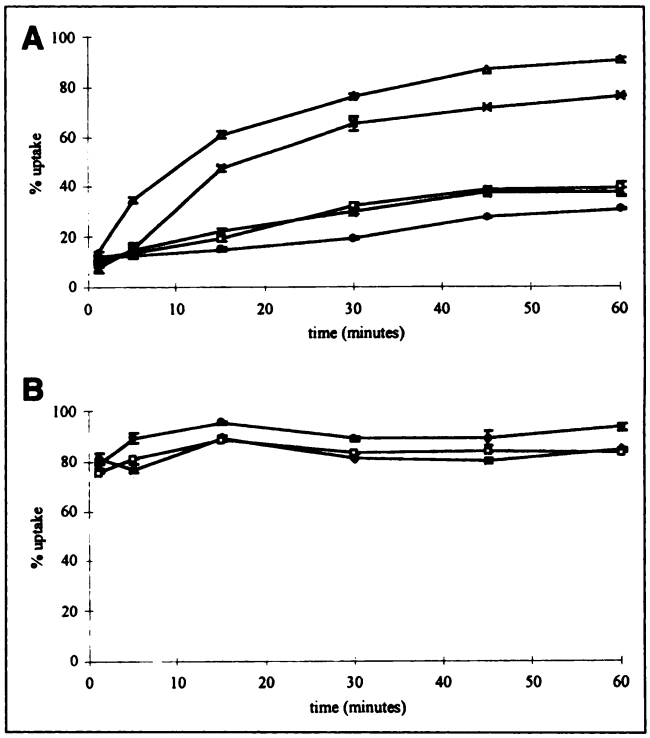

FIGURE 1. Percentage uptake of (A)^{64}Cu-ATSM and (B)^{64}Cu-PTSM into EMT6 cells over time at varying oxygen concentrations: 0% O_2 (△), 0.1% O_2 (X), 0.5% O_2 (▲), 5% O_2 (□) and 20% O_2 (●). Errors if not indicated are within symbols.

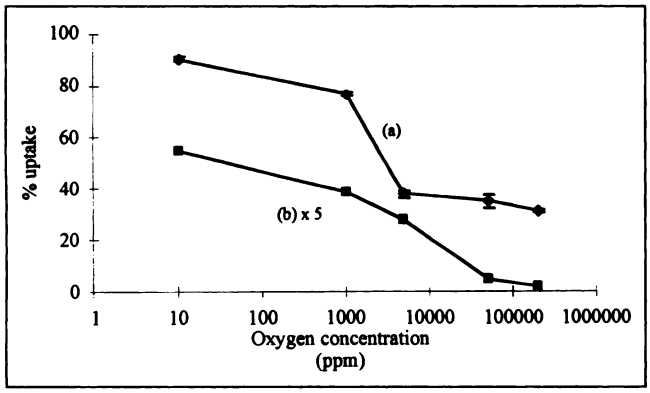

FIGURE 2. (A) Percentage uptake of ^{64}Cu-ATSM (◆) after 1 h against oxygen concentration (expressed in ppm). (B) Percentage uptake of ^{18}F-MISO (■) after 2 h against oxygen concentration (expressed in ppm). Values shown are actual percent multiplied by 5 (for clarity). Errors if not indicated are within symbols.

h, the percentage uptake of ^{18}F-MISO into the cells was seen to be pO_2 dependent, but only approximately 10% of the uptake of ^{64}Cu-ATSM (10.9% at 0 ppm, 7.7% at 1×10^3 ppm, 5.6% at 5×10^3 ppm, 1.0% at 5×10^4 ppm and 0.5% at 2×10^5 ppm) (Fig. 2B).

Washout studies of ^{64}Cu-ATSM and ^{64}Cu-PTSM from the EMT6 cells after 1 h incubation with the tracer at various pO_2 and resuspension in fresh media were performed at 20% O_2. It is clearly seen that the oxygen concentrations during the initial tracer incubation determine the amount of radioactivity washed out from the cells incubated with ^{64}Cu-ATSM (Fig. 3A). Assuming 100% radioactivity associated with the cells at 0 min, after 1 h the cells previously maintained at anoxic (0%) oxygen levels lost 27% of the radioactivity. For cells incubated at 5% O_2, this value was 32% and at normal pO_2 (20% O_2) 42%. The cells incubated with ^{64}Cu-PTSM, however, retained radioactivity independent of the initial pO_2 (Fig. 3B). The amount of radioactivity lost after 1 h was between 9%–11% at all pO_2.

Animal Biodistribution Studies

Biodistributions at 1, 5, 10, 20 and 40 min were performed with ^{64}Cu-ATSM and ^{64}Cu-PTSM (Table 1). Biodistribution of ^{64}Cu-ATSM was also performed at 1, 2 and 4 h (data not shown).

Both ^{64}Cu-ATSM and ^{64}Cu-PTSM are rapidly and efficiently cleared from the blood (3.65%ID/g and 3.82%ID/g, respectively) at 1 min. After 40 min, 2.22%ID/g ^{64}Cu-ATSM and 1.87%ID/g ^{64}Cu-PTSM is still seen in the blood pool. For ^{64}Cu-ATSM over 4 h, this value does not decrease (2.22%ID/g).

^{64}Cu-PTSM is efficiently extracted into the lung (28.69%ID/g) after 1 min and is retained over the 40-min period (30.07%ID/g). Conversely, ^{64}Cu-ATSM exhibits a lower uptake after 1 min (12.89%ID/g) compared with ^{64}Cu-PTSM and is retained over a 4-h period (10.84%ID/g). In the heart tissue after 1 min, 20.50%ID/g ^{64}Cu-PTSM is extracted from the blood pool and retained (16.75%ID/g) over 40 min. ^{64}Cu-ATSM shows markedly smaller extraction values and greater washout from myocardium, 8.75%ID/g at 1 min, lowering significantly to 3.81%ID/g after 40 min ($P < 0.001$) (77% lower than that observed for ^{64}Cu-PTSM).

The brain presents the most suitable control organ for the comparison between ^{64}Cu-ATSM and ^{64}Cu-PTSM. ^{64}Cu-PTSM rapidly crosses the blood-brain barrier and is retained in the brain tissue (*24,25*); 9.38%ID/g ^{64}Cu-PTSM was in the brain after 1 min and stabilized at 8.39%ID/g over 40 min. ^{64}Cu-ATSM, although initially extracted efficiently from the blood pool into the brain (10.46%ID/g at 1 min), is not reduced intracellularly and is washed out, giving values of 3.34%ID/g at 40 min and 2.85%ID/g at 4 h.

Both ^{64}Cu-ATSM and ^{64}Cu-PTSM are cleared through the liver and kidney. Fast kidney uptake is observed for both ^{64}Cu-ATSM (23.45%ID/g at 1 min) and ^{64}Cu-PTSM (28.32%ID/g), decreasing to similar levels after 40 min (11.94%ID/g and 14.48%ID/g, respectively). Liver uptake increases for both complexes over time. ^{64}Cu-ATSM increases from 7.75%ID/g at 1 min to 29.83%ID/g at 40 min, and ^{64}Cu-PTSM increases from 7.21%ID/g at 1 min to 25.70%ID/g at 40 min. Liver uptake is followed by uptake in the intestines before excretion for both compounds. These values stabilize for ^{64}Cu-ATSM over 4 h.

The uptake of ^{64}Cu-ATSM and ^{64}Cu-PTSM into the EMT6 tumor showed optimal uptake after 10 min (4.78 ±

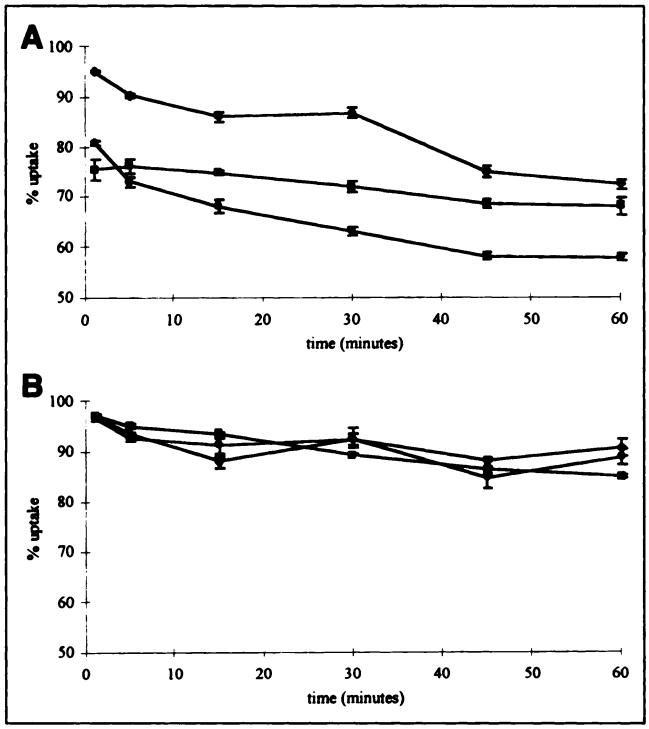

FIGURE 3. Washout of ^{64}Cu-ATSM (A) and ^{64}Cu-PTSM (B) from EMT6 cells after 1 h incubation at 37°C at varying oxygen concentrations; 0% O_2 (◆), 5% O_2 (■), 20% O_2 (●). Errors if not indicated are within symbols.

TABLE 1
Biodistribution (%ID/g ± SD, n = 4) at 1, 5, 10, 20 and 40 min of ^{64}Cu-ATSM (top) and ^{64}Cu-PTSM (bottom) in BALB/c Mice Bearing the EMT6 Mammary Tumor

Tissue	1 min	5 min	10 min	20 min	40 min
Blood	3.65 ± 0.15	2.13 ± 0.37	2.25 ± 0.25	1.79 ± 0.26	2.22 ± 0.15
Lung	12.89 ± 0.55	11.71 ± 0.37	12.21 ± 0.99	11.88 ± 0.95	14.86 ± 1.23
Liver	7.75 ± 1.47	20.84 ± 2.50	22.98 ± 1.43	27.82 ± 1.99	29.83 ± 1.20
Spleen	4.80 ± 1.63	6.86 ± 1.37	6.40 ± 0.60	5.38 ± 0.22	5.24 ± 0.19
Kidney	23.45 ± 1.60	18.02 ± 0.85	17.29 ± 0.36	14.32 ± 0.97	11.94 ± 1.65
Heart	8.75 ± 0.05	4.15 ± 0.59	3.94 ± 0.25	3.26 ± 0.47	3.81 ± 0.42
Brain	10.46 ± 0.41	4.78 ± 0.35	3.76 ± 0.30	3.18 ± 0.16	3.34 ± 0.32
Bone	1.82 ± 0.29	1.64 ± 0.29	1.86 ± 0.38	1.33 ± 0.27	1.47 ± 0.27
Tumor	3.50 ± 0.73	3.41 ± 0.36	4.78 ± 1.00	3.76 ± 0.61	4.17 ± 1.03
Intestines	5.25 ± 0.50	7.87 ± 1.10	9.66 ± 0.19	10.59 ± 1.05	13.34 ± 1.08
Tissue	**1 min**	**5 min**	**10 min**	**20 min**	**40 min**
Blood	3.82 ± 0.29	2.91 ± 0.31	2.28 ± 0.27	1.55 ± 0.26	1.87 ± 0.20
Lung	28.69 ± 4.93	33.14 ± 0.72	34.02 ± 3.19	28.39 ± 4.75	30.07 ± 2.16
Liver	7.21 ± 1.19	12.32 ± 1.00	16.42 ± 1.32	20.84 ± 0.70	25.70 ± 0.68
Spleen	6.25 ± 0.77	4.95 ± 1.05	5.93 ± 0.89	3.54 ± 0.57	4.72 ± 0.56
Kidney	28.32 ± 1.39	21.09 ± 2.53	22.21 ± 4.89	14.83 ± 2.29	14.48 ± 1.32
Heart	20.50 ± 2.36	18.99 ± 5.11	19.04 ± 0.99	14.18 ± 3.65	16.75 ± 1.31
Brain	9.38 ± 0.90	9.04 ± 0.62	10.16 ± 1.19	7.42 ± 0.99	8.39 ± 1.23
Bone	1.48 ± 0.38	1.42 ± 0.33	1.44 ± 0.03	1.37 ± 0.21	1.73 ± 0.28
Tumor	3.35 ± 0.54	3.36 ± 0.69	4.40 ± 1.00	4.34 ± 0.69	4.26 ± 0.81
Intestines	5.77 ± 0.29	5.68 ± 1.14	5.90 ± 0.62	5.03 ± 1.21	6.32 ± 0.70

1.00%ID/g for ^{64}Cu-ATSM and 4.40 ± 1.00%ID/g for ^{64}Cu-PTSM).

Ex Vivo Autoradiography

Ex vivo autoradiography of the EMT6 tumors was undertaken by the co-injection of ^{60}Cu-PTSM and ^{64}Cu-ATSM into the same animal (Fig. 4). The ^{60}Cu-PTSM displays homogeneous uniform uptake throughout the tumor, suggesting uniform blood flow. After allowing for the decay of the shorter lived ^{60}Cu, the ^{64}Cu-ATSM distribution was observed. All tumors studied exhibited heterogeneous uptake of the hypoxic tracer, indicative of the selective trapping of ^{64}Cu-ATSM into the hypoxic cells of the tumor. Figure 4 is representative of the six studies, with intense uptake of ^{64}Cu-ATSM observed in 15%–30% of the tumor.

DISCUSSION

Copper complexes based on thiosemicarbazone ligands have been investigated for use within the field of radiopharmaceutical chemistry (*11,13–15,21,24–27*). One such application is in the selective detection of viable hypoxic tissue. Cu-ATSM has been investigated for the detection of heart ischemia (*15*). The successful determination of the hypoxic fraction within a tumor is important when considering a treatment regimen with radiotherapy or chemotherapy (*3*). Cu-ATSM is a complex of low molecular weight, high membrane permeability and low redox potential for selective retention within hypoxic tissue. Therefore, the use of Cu-ATSM in the detection of tumor hypoxia is of significant clinical interest. We report here our findings on the selectivity of Cu-ATSM for hypoxic tissue in comparison with ^{64}Cu-PTSM,

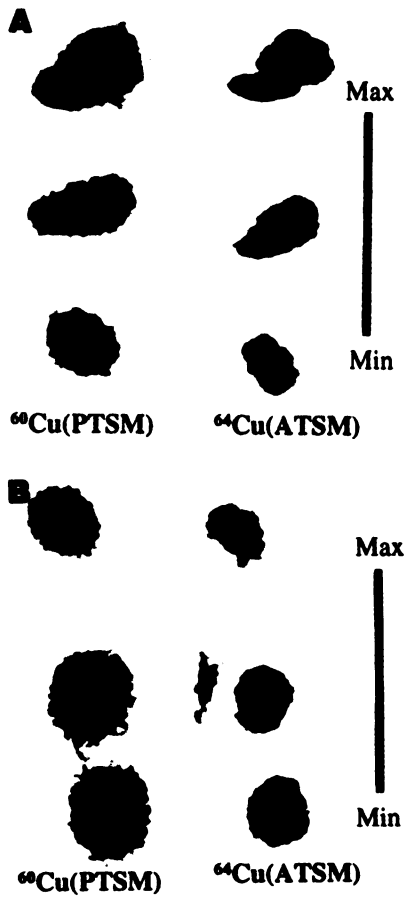

FIGURE 4. (A)Typical autoradiograph of EMT6 tumor with ^{60}Cu-ATSM (right) and ^{64}Cu-PTSM (left). (B) Typical autoradiograph of EMT6 tumor with ^{60}Cu-ATSM (right) and ^{64}Cu-PTSM (left).

a known blood-flow and tumor-flow tracer (*24,25*), and ^{18}F-MISO, a known tracer for the detection of hypoxic tissue (*28–30*).

The EMT6 carcinoma cell line is an in vitro cultured cell line available in monolayer, spheroidal and in vivo form (*31, 32*). This cell line has been used extensively to investigate hypoxic agents, because the cells cultured as spheroids or as solid tumors in vivo in BALB/c mice contain a significant hypoxic fraction dependent on size and age (*33,34*).

The apparatus used in the in vitro experiments was designed to provide the cells with a controlled environment. The use of 5% CO_2 in all the certified gas mixtures preserved the pH of the media, and the continual agitation of the cells avoided clumping and possible formation of spheroidal microenvironments. Cell concentration, although not directly investigated as a determining factor in compound uptake in this investigation, was maintained at constant levels. The maintenance of temperature and cell density/concentration ensures that these factors do not contribute to differences in uptake between the compounds investigated, an observation noted in an investigation on the technetium-labeled nitroimidazole derivative-BMS181321 (*11*). The gases were warmed and humidified by passing through a glass bubbler that contained water at 37°C. The glass vessels and Tygon R3603 tubing (Norton, Akron, Ohio) were used in the apparatus because of their relative impermeability to oxygen. Therefore, the uptake of radiolabeled compound is entirely based on the dissolved pO_2 in the cell media.

In the in vitro study, the uptake of ^{64}Cu-ATSM is related in a sigmoidal fashion to the pO_2 of the media, where retention was markedly increased under hypoxic and anoxic conditions (Fig. 2A). The uptake of ^{18}F-MISO in the EMT6 cells in monolayers follows a similar pattern (Fig. 2B). This same binding profile is observed for the uptake of [^{3}H]F-MISO into EMT6 and V79 cells (*35,36*). With ^{18}F-MISO, binding to the EMT6 cells initiates at higher oxygen concentrations than with ^{64}Cu-ATSM. The percentage uptake of ^{18}F-MISO is also much lower than that of ^{64}Cu-ATSM after a longer incubation time. It was necessary to use monolayers of cells at a higher concentration to show the oxygen-dependent binding of ^{18}F-MISO to EMT6 cells. The significance of the much lower cellular uptake of ^{18}F-MISO and the uptake at different pO_2 to in vivo situations has yet to be determined. ^{64}Cu-PTSM showed uptake completely independent of oxygen concentration. From Figure 1a, it is seen that ^{64}Cu-ATSM is selectively trapped at levels depending on the pO_2. The significant ($P < 0.01$) and equal uptake of the flow tracer, ^{64}Cu-PTSM, at all oxygen concentrations, acts as a suitable control to ^{64}Cu-ATSM.

The difference in retention between Cu-ATSM and Cu-PTSM is due to the different redox potentials of the complexes. Minkel et al. (*37*) reported the redox potential of Cu-PTSM (−208 mV), and Fujibayashi et al. (*15*) published the redox potential of Cu-ATSM (−297 mV). Taniuchi et al. (*27*) have reported that Cu-PTSM is reduced at the Complex I site of the electron transport chain using NADH as the electron donor. NADH has a redox potential of −315 mV (*38*), similar to that of Cu-ATSM. Cu-ATSM, with a redox potential 89 mV lower than that of Cu-PTSM, is reduced less efficiently at the Complex I site under the same conditions (*15*). Under hypoxic conditions, depletion of oxygen causes hyper-reduction of Complex I and an increase in NADH concentration (*39*). This accounts for the difference in uptake and retention between ^{64}Cu-ATSM and ^{64}Cu-PTSM. This is observed in the EMT6 cell uptake studies, since under hypoxic conditions, the cells would contain Complex I with particularly high electron and/or NADH concentrations.

Others researchers have suggested that ubiquitous sulfhydryl (SH) groups, such as glutathione (GSH), are responsible for the retention of Cu-PTSM in normal cells (*24,25,40*). It would be reasonable to assume that under hypoxic conditions, the retention of Cu-ATSM is due to enzymatic reduction, most probably at the Complex I site as discussed previously.

The washout studies further support this hypothesis. ^{64}Cu-PTSM is reduced and trapped in all cells, and therefore little washout from the cells is observed when the media is changed (<11%) (Fig. 3B). With ^{64}Cu-ATSM, over 42% of the complex is washed out from the normoxic cells after 1 h. In hypoxic cells, this value is only 27%, suggesting the selective retention of the complex in a more reducing cellular environment (Fig. 3A). Fujibayashi et al. (*15*) confirmed this observation, in that hypoxic retention of Cu-ATSM is a reversible phenomenon dependent only on pO_2 and not on irreversible cellular damage such as membrane disruption.

^{18}F-MISO, although used for the detection of hypoxic tissue, has two disadvantages: low cellular uptake and slow washout from normoxic tissue (*29*). This is demonstrated by the in vitro uptake studies in which, over a 1-h period, less than 2% of ^{18}F-MISO was taken up by the EMT6 at any pO_2. After 2 h, binding of the tracer was seen to be dependent on oxygen concentration in EMT6 cells at higher cell concentrations (Fig. 2B). However, the more efficient uptake and washout kinetics of ^{64}Cu-ATSM in hypoxic and normoxic cells offers the possibility of a fast and efficient means of detecting tumor hypoxia by PET imaging. Currently, clinical studies involving ^{18}F-MISO produce images showing differences between normal and hypoxic tissues but only hours postinjection as a result of slow blood clearance and low tumor-to-muscle ratios (*29,30,41*).

Both ^{64}Cu-ATSM and ^{64}Cu-PTSM are small neutral, lipophilic, square planar compounds that can easily transverse the blood-brain barrier (*14,24*). Both ^{64}Cu-ATSM and ^{64}Cu-PTSM were extracted rapidly from the blood compartment. The major organs such as the lung, brain and kidney showed efficient extraction and retention of the flow tracer ^{64}Cu-PTSM as already described (*24,25*). The extraction of ^{64}Cu-ATSM at 1 min was either equal or less efficient than ^{64}Cu-PTSM. The heart and brain extraction of ^{64}Cu-PTSM was followed by retention of the complex over the 40-min

experimental period. ^{64}Cu-ATSM showed similar initial uptake compared with ^{64}Cu-PTSM but cleared from these organs over the 40-min period.

In the in vitro experiments, the initial uptake of ^{64}Cu-ATSM into the EMT6 cells is slower than that of ^{64}Cu-PTSM. However, in the biodistribution experiments, the rate of extraction of ^{64}Cu-ATSM into the tumor and brain is similar to that of ^{64}Cu-PTSM at 1 min. The extraction of the tracers into tissues in vivo may be on a faster time scale than 1 min. Moreover, the extraction will also be faster because of the significantly higher concentration of cells in vivo.

^{64}Cu-PTSM has been shown to measure tumor blood flow (*26*), and this is confirmed in this EMT6 animal model. The data suggest equal uptake of ^{64}Cu-ATSM and ^{64}Cu-PTSM in the EMT6 tumors when comparing %ID/g values. It is difficult to determine whether this similarity in uptake is due to a high hypoxic fraction in these tumors and therefore equal extraction and retention of ^{64}Cu-PTSM and ^{64}Cu-ATSM from the blood pool or distinct changes in blood flow and tumor morphology. It is also possible that ^{64}Cu-ATSM is retained in the hypoxic regions at a greater concentration than ^{64}Cu-PTSM in normal tissue.

Ex vivo autoradiography was undertaken by the co-injection of ^{60}Cu-PTSM and ^{64}Cu-ATSM into the same animal. The validation of dual tracer experiments with the electronic autoradiography system have been reported (*20*). It was shown that the electronic autoradiography system (Packard InstantImager) showed good linearity over a wide range of counts, making it an ideal instrument for ex vivo imaging of positron-emitting radionuclides of different half-lives. The tumors used in this study were smaller than those used in the biodistribution study and contain a smaller hypoxic fraction, due to more efficient blood flow to interior regions of the tumor. The EMT6 tumors were excised after 10 min and sliced for ex vivo imaging by electronic autoradiography (Fig. 4). The ^{60}Cu-PTSM displayed uniform uptake throughout the tumor confirming uniform blood flow. After allowing for the decay of the shorter lived ^{60}Cu, the ^{64}Cu-ATSM distribution was observed. The tumors exhibited heterogeneous uptake of ^{64}Cu-ATSM, indicative of the selective trapping of this tracer into hypoxic cells of the tumor. From the autoradiographs, hypoxic fractions from 15%–45% were observed, values consistent with the expected hypoxic fraction observed for this age of tumor in vivo (*34*).

CONCLUSION

^{64}Cu-ATSM has been shown to be effective in the delineation of hypoxic tumor tissue. Cu-ATSM was selectively trapped in vitro in EMT6 cells under hypoxic conditions and in vivo in solid EMT6 tumors. The fast and selective uptake of Cu-ATSM in hypoxic tissue will allow rapid quantitative and qualitative detection of hypoxic regions in tumors with PET before a radiotherapy or chemotherapy regime.

ACKNOWLEDGMENTS

We thank Michael E. Cristel and Elizabeth L.C. Sherman for assistance in the cell culture and animal studies, Lynne A. Jones and Margaret M. Morris for their technical help in the animal studies, and Todd A. Perkins and Bill Margenaeu for their assistance in the production of ^{64}Cu/^{60}Cu. We also thank Joanna B. Downer for her excellent proofreading of this manuscript and Dr. Carolyn J. Anderson and Jason L. J. Dearling for valuable ideas and discussions. We also wish to express our sincere gratitude to Drs. Ronald S. Pardini and Sandra Johnson of the Department of Biochemistry, University of Nevada, Reno, for their supply of the EMT6 cell line. This work was supported by Department of Energy grant DE-FG02-87ER60512 and National Institutes of Health grant 2-PO1-HL-13851-32.

REFERENCES

1. Coleman CN. Hypoxia in tumors: a paradigm for the approach to biochemical and physiological heterogeneity. *J Natl Cancer Inst.* 1988;80:310–317.
2. Peters LJ, Withers HR, Thames HD, Fletcher GH. Keynote address—the problem: tumor radioresistance in clinical radiotherapy. *Int J Radiat Oncol Biol Phys.* 1982;8:101–108.
3. Moulder JE, Rockwell S. Tumor hypoxia: its impact on cancer therapy. *Br J Radiol.* 1987;26:638–648.
4. Rockwell S, Keyes SR, Sartorelli AC. Preclinical studies of porfiromycin as an adjunct to radiotherapy. *Radiat Res.* 1988;116:100–113.
5. Rockwell S. Effect of some proliferative and environmental factors on the toxicity of mitomycin C to tumor cells in vitro. *Int J Cancer.* 1986;38:229–235.
6. Parliament MB, Chapman JD, Urtasun RC. Non-invasive assessment of human tumour hypoxia with ^{123}I-iodoazomycin arabinoside: preliminary report of a clinical study. *Br J Cancer.* 1992;65:90–95.
7. Grosher D, McEwan AJB, Parliament MB, et al. Imaging tumor hypoxia and tumor perfusion. *J Nucl Med.* 1993;34:885–888.
8. Ng CK, Sinusas AJ, Zaret B, Souter R. Kinetic analysis of technetium-99m-labeled nitromidazole (BMS181321) as a tracer of myocardial hypoxia. *Circulation.* 1995;92:1261–1268.
9. Rumsey WL, Patel B, Linder K. Effect of graded hypoxia in retention of technetium-99m-nitroheterocycle in perfused rat hearts. *J Nucl Med.* 1995;36:632–636.
10. Martin GV, Biskupiak JE, Caldwell JH, Rasey JS, Krohn KA. Characterization of iodovinylmisonidazole as a marker for myocardial hypoxia. *J Nucl Med.* 1993;34:918–924.
11. Ballinger JR, Wan Min Kee J, Rauth AM. In vitro and in vivo evaluation of a technetium-99m-labeled 2-nitroimidazole (BMS181321) as a marker of tumor hypoxia. *J Nucl Med.* 1996;37:1023–1031.
12. Cook GJR, Houston S, Barrington SF, Fogelman I. Technetium-99m-labeled HL91 to identify tumor hypoxia: correlation with fluorine-18-FDG. *J Nucl Med.* 1998;39:99–103.
13. Blower PJ, Lewis JS, Zweit J. Copper radionuclides and radiopharmaceuticals in nuclear medicine. *Nucl Med Biol.* 1996;23:957–980.
14. Taniuchi H, Fujibayashi Y, Yonekura Y, Konishi J, Yokoyama A. Hyperfixation of copper-62-PTSM in rat brain after transient global ischemia. *J Nucl Med.* 1997;38:1130–1134.
15. Fujibayashi Y, Taniuchi H, Yonekura Y, Ohtani H, Konishi J, Yokoyama A. Copper-62-ATSM: a new hypoxia imaging agent with high membrane permeability and low redox potential. *J Nucl Med.* 1997;38:1155–1160.
16. Takahashi N, Fujibayashi Y, Yonekura Y, et al. Evaluation of copper-62 ATSM in patients with lung cancer as a hypoxic tissue tracer [Abstract]. *J Nucl Med.* 1998;39:53P.
17. McCarthy DW, Shefer RE, Klinkowstein RE, et al. Efficient production of high specific activity ^{64}Cu using a biomedical cyclotron. *Nucl Med Biol.* 1997;24:35–43.
18. Bass LA, McCarthy DW, Jones LA, et al. High purity production and potential applications of copper-60 and copper-61. *J Label Comp Radiopharm.* 1997;40:325–327.
19. McCarthy TJ, Dence CS, Welch MJ. Application of microwave heating to the synthesis of [^{18}F]fluoromisonidazole. *Appl Radiat Isot.* 1993;44:1129–1132.

20. Fujibayashi Y, Cutler CS, Anderson CJ, et al. Comparative imaging studies of ^{64}Cu-ATSM a hypoxia imaging agent and C-11-acetate in an acute myocardial infarction model: ex vivo imaging in rats. *Nucl Med Biol.* in press.
21. Young H, Carnochan P, Zweit J, Babich J, Cherry S, Ott R. Evaluation of copper(II)-pyruvaldehyde bis(*N*-4-methylthiosemicarbazone) for tissue blood flow measurement using a trapped tracer model. *J Nucl Med.* 1994;21:336–341.
22. Lewis JS. Phosphine ligands as a basis for copper radiopharmaceutical chemistry. [PhD thesis]. Canterbury, United Kingdom: The University of Kent at Canterbury; 1996.
23. Dearling JLD, Lewis JS, Mullen GED, Rae MT, Zweit J, Blower PJ. Design of hypoxia-targeting radiopharmaceuticals: Selective uptake of copper-64 complexes in hypoxic cells in vitro. *Eur J Nucl Med.* 1998;25:788–792.
24. Green MA. A potential copper radiopharmaceutical for imaging the heart and brain: Copper-labeled pyruvaldehyde bis(N^4-methylthiosemicarbazone). *Nucl Med Biol.* 1987;14:59–61.
25. Green MA, Mathias CJ, Welch MJ, et al. Copper-62-labeled pyruvaldehyde *bis*(*N*^{4}-methylthiosemicarbazone)copper(II): synthesis and evaluation as a positron emission tomography tracer for cerebral and myocardial perfusion. *J Nucl Med.* 1990;31:1989–1996.
26. Mathias CJ, Welch MJ, Perry DJ, et al. Investigation of copper-PTSM as a PET tracer for tumor blood flow. *Nucl Med Biol.* 1991;18:807–811.
27. Taniuchi H, Fujibayashi Y, Okazawa H, Yonekura Y, Konishi J, Yokoyama A. Cu-pyruvaldehyde-bis(*N*^{4}-methylthiosemicarbazone) (Cu-PTSM), a metal complex with selective NADH-dependent reduction by complex I in brain mitochondria: a potential radiopharmaceutical for mitochondria-functional imaging with positron emission tomography. *Biol Pharm Bull.* 1995;18:1126–1129.
28. Koh W-J, Rasey JS, Evans ML. Imaging of hypoxia in human tumors with [F-18]fluoromisonidazole. *Int J Radiat Oncol Biol Phys.* 1992;22:199–212.
29. Shelton ME, Dence C, Hwang D-R, Welch MJ. Myocardial kinetics of fluorine-18 misonidazole: a marker of hypoxic myocardium. *J Nucl Med.* 1989;30:351–358.
30. Martin GV, Caldwell JH, Graham MM, et al. Non-invasive detection of hypoxic myocardium using fluorine-18-fluoromisonidazole and positron emission tomography. *J Nucl Med.* 1992;33:2202–2208.
31. Rockwell S. *In vivo–in vitro* tumor systems: new models for studying the response of tumors to therapy. *Lab Animal Sci.* 1977;27:831–851.
32. Shibamoto Y, Nishimoto S, Mi F, Sasai K, Kagiya T, Abe M. Evaluation of various types of new hypoxic cell sensitizers using the EMT6 single cell-spheroid-solid tumor system. *Int J Radiat Biol.* 1987;52:347–357.
33. Franko AJ. Hypoxic fraction and binding of misonidazole in EMT6/Ed multicellular tumor spheroids. *Radiat Res.* 1985;103:89–97.
34. Moulder JE, Rockwell S. Hypoxic fractions of solid tumors: experimental techniques, methods of analysis, and a survey of existing data. *Int J Radiat Oncol Biol Phys.* 1984;10:695–712.
35. Rasey JS, Wui-Jin K, Grierson JR, Grunbaum Z, Krohn KA. Radiolabeled fluoromisonidazole as an imaging agent for tumor hypoxia. *Int J Radiat Oncol Biol Phys.* 1989;17:985–991.
36. Rasey JS, Nelson NJ, Chin L, Evans ML, Grunbaum Z. Characteristics of the binding of labeled fluoromisonidazole in cells *in vitro*. *Radiation Res.* 1990;122: 301–308.
37. Minkel DT, Saryan LA, Petering DH. Structure-function correlations in the reaction of bis(thiosemicarbazonato) copper(II) complexes with Ehrlich ascites tumor cells. *Cancer Res.* 1978;38:124–129.
38. McGilvery RW, Goldstein GW. Oxidations and phosphorylations. In: McGilvery RW, ed. *Biochemistry, A Functional Approach.* 3rd ed. Philadelphia, PA: WB Saunders; 1983:390–420.
39. Barlow CH, Harken AH, Chance B. Evaluation of cardiac ischemia by NADH fluorescence photography. *Ann Surg.* 1977;186:737–740.
40. Barnhart-Bott A, Green MA. The effects of glutathione depletion on the biodistribution of Cu(PTSM) in rats. *Nucl Med Biol.* 1991;18:865–869.
41. Nunn A, Linder K, Strauss HW. Nitroimidazoles and imaging hypoxia. *Eur J Nucl Med.* 1995;22:265–280.